

Yeast mitochondrial protein Pet111p binds directly to two distinct targets in *COX2* mRNA, suggesting a mechanism of translational activation

Julia L. Jones^{1,2}, Katharina B. Hofmann³, Andrew T. Cowan^{2#}, Dmitry Temiakov⁴, Patrick Cramer³, and Michael Anikin^{2*}

From the ¹Graduate Program in Cell and Molecular Biology, Graduate School of Biomedical Sciences and ²Department of Cell Biology & Neuroscience, Rowan University School of Osteopathic Medicine, 42 East Laurel Road, UDP 2200, Stratford NJ 08084, USA; ³Department of Molecular Biology, Max Planck Institute for Biophysical Chemistry, 37077 Göttingen, Germany; ⁴Department of Biochemistry & Molecular Biology, Sidney Kimmel Cancer Center, Thomas Jefferson University, 1020 Locust Street, Philadelphia PA 19107

Running title: *Translational activator Pet111p interacts with COX2 mRNA*

[#]Present address: Department of Pharmacy, Thomas Jefferson University Hospital, 111 South 11th Street, Suite 2260, Philadelphia PA 19107

*To whom correspondence should be addressed: Michael Anikin: Department of Cell Biology & Neuroscience, Rowan University School of Osteopathic Medicine, Stratford NJ 08084; anikinmi@rowan.edu; Tel. (856) 566-6326; Fax. (856) 566-2881.

Keywords: mitochondria, cytochrome *c* oxidase, gene expression, RNA-protein interaction, translation regulation, translational activator, pentatricopeptide repeat (PPR) protein, respiratory complex, PAR-CLIP

ABSTRACT

The genes in mitochondrial DNA code for essential subunits of the respiratory chain complexes. In yeast, expression of mitochondrial genes is controlled by a group of gene-specific translational activators encoded in the nucleus. These factors appear to be part of a regulatory system that enables concerted expression of the necessary genes from both nuclear and mitochondrial genomes to produce functional respiratory complexes. Many of the translational activators are believed to act on the 5'-untranslated regions of target mRNAs, but the molecular mechanisms involved in this regulation remain obscure. In this study, we used a combination of *in vivo* and *in vitro* analyses to characterize the interactions of one of these translational activators, the pentatricopeptide repeat (PPR) protein Pet111p, with its presumed target, *COX2* mRNA, which encodes subunit II of cytochrome *c* oxidase. Using photoactivatable ribonucleoside-enhanced crosslinking and immunoprecipitation (PAR-CLIP) analysis, we found that Pet111p binds directly and specifically to a 5'-end proximal

region of the *COX2* transcript. Further, we applied *in vitro* RNase footprinting and mapped two binding targets of the protein, one of which is located in the 5'-untranslated leader and the other within the coding sequence. Combined with available genetic data, these results suggest a plausible mechanism of translational activation, in which binding of Pet111p may prevent inhibitory secondary structures from forming in the translation initiation region, thus rendering the mRNA available for interaction with the ribosome.

The yeast cytochrome *c* oxidase (COX) complex is an assembly of 12 subunits (1), of which only three, Cox1p, Cox2p, and Cox3p, are encoded by mitochondrial DNA (mtDNA), while the others are the products of nuclear genes. A regulatory system must therefore be in place to ensure coordinated expression from both genomes, such that all of the subunits are produced synchronously and stoichiometrically for the correct assembly of the complex (2). This system appears to utilize a set of nuclear DNA-encoded

messengers that act in a gene-selective manner to authorize the mitochondrial mRNAs to undergo translation (2-4). Expression of subunit II of COX, Cox2p, is under the control of one of such messengers, the product of the nuclear gene *PET111* (5,6). Genetic characterization has demonstrated that the product of this gene, Pet111p, sanctions the translation of *COX2* by acting in the 5'-UTR of the mRNA (7) and thereby limits the production of Cox2p under physiologic conditions (8). As is the case with most yeast mitochondrial gene-specific translational activators (3), Pet111p is anchored to the matrix surface of the inner mitochondrial membrane, thus enabling co-translational insertion of the nascent Cox2p into the membrane (8). This function of Pet111p appears to be of critical importance because Cox2p failed to accumulate when translated away from the membrane (9). At the membrane, Pet111p is associated in a complex, which also includes translational activators specific to *COX1*, *COX3*, and *COB* (10,11). This suggests an additional function of the translational activators to ensure proper spatial coordination during the production and assembly of respiratory complexes III and IV. All of these interactions presumably take place in the framework of the recently discovered MIOREX super complex, which is responsible for the organization of mitochondrial gene expression (12).

The finding that Pet111p functionally interacts with the 5'-UTR of *COX2* (7,13) to enable translation invited a suggestion that the protein may bind to the mRNA directly. However, a direct binding of Pet111p to *COX2*, or any other RNA, has not yet been demonstrated. In this study, we evaluated Pet111p for its potential to interact with RNA both *in vivo* and *in vitro*. Using photoactivatable ribonucleoside-enhanced crosslinking and immunoprecipitation (PAR-CLIP) analysis, we confirmed that Pet111p preferentially associates with the 5'-end proximal portion of *COX2* mRNA. Further analysis by a combination of electrophoretic mobility shift assay (EMSA) and RNase footprinting revealed two distinct binding targets of the protein, one close to the 5'-end of the transcript and one in the beginning of the coding sequence. Based on the positions of the binding targets and taking into account the results of genetic analysis and the prediction of the structural organization of the

RNA, we suggest plausible mechanisms by which binding of Pet111p could facilitate translation of *COX2*.

Results

Pet111p directly contacts *COX2* mRNA *in vivo*

To examine if Pet111p is engaged in direct contacts with RNA *in vivo*, we carried out an unbiased analysis using PAR-CLIP. Yeast expressing tandem affinity purification (TAP) tagged Pet111p (Pet111p-TAP) were grown in the presence of 4-thiouracil (4tU) and UV-irradiated to induce the formation of RNA-protein cross-linking products. The cells were then lysed and the lysate was subjected to immunoprecipitation (IP) using anti-TAP-tag antibodies. The co-precipitated RNA species were trimmed with RNase T1 and the presence of Pet111p-TAP in the resulting immunoprecipitate was confirmed by western blotting (Figure S1). The photo cross-linked RNA in a part of the sample was 5'-[³²P]-labeled and analyzed by SDS PAGE. As shown in Figure S1, a population of radioactive species with an electrophoretic mobility approximately corresponding to Pet111p-TAP was dominant on the gel. We interpreted these species as RNA-Pet111p-TAP cross-linking products. After adapter ligation, the cross-linked RNA was converted into cDNA, PCR-amplified, and the amplification products were subjected to deep sequencing. The collected sequencing reads 20-50 nucleotides (nt) in length aligned with the sequence of mtDNA are presented in Figure 1A. The alignment showed that the vast majority of the reads belonged to *COX2* mRNA. While some background levels of the RNA in the sample originated from the nuclear genome or represented other mitochondrial genes, the RNA sequences associated with *COX2* were over 30 times more abundant (Figure 1B). Within the *COX2* mRNA (Figure 1C), the density of the reads was significantly higher in the 5'-end proximal region, including the 5'-UTR and approximately 60 nucleotides into the beginning of the coding sequence. These results confirm that Pet111p is indeed an RNA binding protein that selectively interacts with *COX2* *in vivo* with a particularly high affinity to the 5'-end region of the mRNA.

Expression of recombinant *Pet111p*

To determine whether Pet111p requires additional mitochondrial factors to bind to *COX2* and to define its binding target (or targets) with greater precision, we purified a recombinant form of the protein and used it to assemble and evaluate complexes with synthetic RNA oligonucleotides of defined length and sequence.

As is the case for most nucleus-encoded mitochondrial proteins, Pet111p is expected to undergo N-terminal processing during import into mitochondria. We intended to generate a recombinant form of the mature protein; however to the best of our knowledge the processing site of Pet111p has never been experimentally established. To determine the site of maturation, we took advantage of an available library of yeast ORFs inserted into the BG1805 expression vector (14) that provides a C-terminally fused hexahistidine tag. We overexpressed the tagged Pet111p in yeast, isolated the mitochondrial fraction, and partially purified the processed form of the protein using Ni-IDA beads under denaturing conditions. Analysis of the preparation by PAGE (Figure 2A) revealed a major band running at approximately 97 kDa and the protein in the band was further identified as Pet111p by peptide mass fingerprinting (PMF) (15). Edman degradation analysis of the protein returned two overlapping sequences, STELI and YSTEL. We therefore concluded that Pet111p undergoes a two-step processing with mitochondrial processing peptidase (MPP) cleaving a 33 amino acid peptide at Y33 and Icp55p removing residue Y34 (Figure 2A). Based on these data, we constructed a plasmid for bacterial expression of a mature form of Pet111p, in which an N-terminal histidine purification tag (MAH₆) was fused to amino acid S35 of the protein. This recombinant form of the protein is referred to as rPet111p in this study. Expression in *E. coli* at a reduced temperature and low induction levels allowed us to obtain rPet111p in a soluble form. The protein was purified to homogeneity by a preliminary enrichment with Ni-IDA beads followed by heparin affinity chromatography and gel filtration (Figure S2A). Surprisingly, the apparent electrophoretic mobility of rPet111p corresponded to a molecular weight of approximately 70 kDa, which was substantially lower than the calculated value of 91.3 kDa. To exclude that this shift was due to a truncation that might have occurred during the expression, we

determined the actual molecular weight of the protein in the preparation by MALDI TOF mass spectrometry. As shown in Figure S2B, the observed molecular weight of rPet111p was in agreement with the expected value.

COX2 mRNA does not undergo maturation at the 5'-end

Several yeast mitochondrial mRNAs have been shown to undergo Pet127p-dependent trimming at the 5'-end following endonucleolytic processing of the primary transcripts (16). The position of the 5'-end in mature *COX2* was previously mapped to coincide with the start site of the *COX2* promoter (17). The mapping was performed at a single-nucleotide resolution by extension of a DNA primer hybridized to *COX2* with reverse transcriptase (RT). However, the 3'-end of the primer used in the study corresponded to position 33 inside the 5'-UTR and thus, had the trimming shifted the 5'-end into the region between that point and the translational start site, the experiment would fail to detect the maturation product. Therefore, to design the RNA oligonucleotides for the *in vitro* reconstruction of the rPet111p-RNA complexes, we needed to verify the position of the 5'-end in mature *COX2*. We repeated the primer extension experiment shifting the entire primer to a location inside the coding sequence. As shown in Figure 2B, extension of the primer did not terminate near the area of the initiation codon and produced a larger single product. Comparison with a set of DNA size markers placed the 3'-end of the product to the position corresponding to +1 of the primary transcript, consistent with published data (17). This allowed us to conclude that *COX2* does not undergo a 5'-end trimming, and thus the entire sequence of its 5'-UTR was included in the evaluation of interaction with rPet111p.

rPet111p specifically binds in vitro to at least two distinct targets in the 5'-end proximal region of COX2

Our PAR-CLIP analysis showed that Pet111p interacts with RNA directly and specifically *in vivo*. To examine whether the protein retains this ability in the absence of other mitochondrial factors, we used EMSA. In this experiment, radioactively labeled RNA probes of defined sequence were incubated with rPet111p to

allow the formation of complexes, which were then separated from free RNA by native PAGE. We first compared two RNA probes, of which one encompassed the entire *COX2* 5'-UTR (*COX2*-1-54) and the other represented a sequence downstream from the coding sequence (nonspecific control, NSC). As shown in Figure 3A, EMSA revealed prominent bands corresponding to the *COX2*-1-54-rPet111p complex whereas NSC failed to complex appreciably with the protein. We conclude that rPet111p can discriminate between RNA molecules independently of other mitochondrial proteins, and that the 5'-UTR harbors a binding target of the protein.

A relatively stable stem-loop structure has been predicted to form upstream of the ORF of *COX2* (18). It resides within a 31-nt region, which has been shown to contain residues required for respiration (19), suggesting that the stem-loop might be a target of Pet111p. To evaluate this possibility, we used an overlapping pair of RNA probes, which covered the entire sequence of the 5'-UTR, but were positioned in such a way that the stem-loop structure could not form in either probe. If this structure was required for binding to Pet111p, we would expect to see a loss of the complex formation with both probes. However as shown in Figure 3B, while the *COX2*-23-54 probe failed to form a complex, the 5'-end proximal probe (*COX2*-1-30) retained the ability to interact with the protein. These results indicate that a binding target of Pet111p resides within the sequence of *COX2*-1-30 and argue against the involvement of the stem-loop as a major binding or specificity determinant. Considering that no secondary structure is expected to form within *COX2*-1-30, Pet111p can thus be classified as a sequence-specific single-stranded RNA binding protein.

The high abundance of the PAR-CLIP sequencing reads at the site of translation initiation of *COX2* (Figure 1C) prompted us to examine whether that region had an additional binding target for Pet111p. The probe used in this experiment (*COX2*-58-95) extended from just downstream of the initiation codon to the descending strand of a predicted stem-loop structure (20) located in the beginning of the coding sequence. EMSA revealed that this probe could readily complex with rPet111p with an

affinity comparable to that of the *COX2*-1-30 probe, which was used as a positive control (Figure 3C). Therefore we conclude that at least two Pet111p binding targets are present in the 5'-end proximal region of *COX2*, one in the beginning of the 5'-UTR and one downstream from the initiation codon, and that the protein can recognize both targets independently of other mitochondrial factors.

The two mapped RNA targets of Pet111p share little similarity

Our EMSA results indicated the presence of Pet111p binding targets in the RNA probes *COX2*-1-30 and *COX2*-58-95. To define the targets with greater precision, we employed RNase I footprinting (21). 5'-[³²P]-labeled *COX2*-1-30 was subjected to limited digestion with RNase I, and the products of digestion were separated at a single-nucleotide resolution (Figure 4A, lane 2). RNase I is known to cleave poorly at GMP residues (22), and thus the weak band corresponding to the product of cleavage at G22 was readily identifiable and provided a reference point to assign other bands in the lane. The pattern of the cleavage products was reasonably uniform throughout the probe, except at the purine-rich 3'-end where the cleavage was somewhat less prominent, suggesting that the probe was free of secondary structures. The probe was also incubated with rPet111p to allow the formation of a complex, the complex was treated with RNase I, and the products of digestion were separated (Figure 4A, lane 3). The pattern of the cleavage was clearly different in the presence of rPet111p. As evident from the traces representing the distribution of radioactivity in lanes 2 and 3, the cleavage efficiency decreased drastically in a region close to the middle of the probe while increasing towards the ends. For each RNA fragment 2 to 29 nt in length, the effect of rPet111p was plotted as a logarithm of the intensity ratio in lanes 2 and 3 (bar plot in Figure 4A). The positive-value bars in the plot indicated the residues in the RNA, at which RNase I cleavage was partially blocked by rPet111p. The most prominent protection was observed between positions 7 and 19, suggesting the presence of a Pet111p binding target within these boundaries. In a similar way, probe *COX2*-58-95 was subjected to RNase I in the absence or presence of rPet111p

(Figure 4B). The cleavage products were quantified and analyzed as described above and a region between positions 66 and 85 was identified as partially protected by the protein, which defined the boundaries of a second binding target of rPet111p. The clear footprints observed with both RNA probes attested once again to the ability of rPet111p to discriminate in favor of certain sequences in a single-stranded RNA context. As shown in Figure 4C, the positions of the two mapped targets correlated with the areas in the *COX2* mRNA where the PAR-CLIP sequence reads were the most abundant. Interestingly, the peaks of the density of the reads were somewhat shifted downstream relative to the rPet111p binding targets, probably reflecting a bias imposed by the PAR-CLIP method.

The finding that the two mapped targets of rPet111p substantially differ in length (13 nt versus 21 nt in the 5'-UTR and ORF targets, respectively) and share little sequence similarity was surprising. To account for this observation, one can assume that Pet111p might harbor two RNA binding sites, of which each recognizes one of the two targets. Hypothetically, the protein could then associate with both targets simultaneously if the two binding sites worked independently. To test if this was the case, we used EMSA to resolve the complexes that were formed by rPet111p in the presence of both *COX2*-1-30 and *COX2*-58-95 (Figure 4D). In the first set of samples, the radiolabeled probe *COX2*-1-30 was present at a fixed concentration while the concentration of *COX2*-58-95, which was not labeled, was gradually increased. Due to the basic nature of the protein, the electrophoretic mobility of the complexes is mostly controlled by their charge. Thus, within the range of the lengths of the RNA probes used in the study, the longer the RNA associated with rPet111p, the greater the mobility of the complex. Accordingly, if the *COX2*-58-95 probe were to bind to the radiolabeled *COX2*-1-30-rPet111p binary complex, the radioactive band of this ternary complex would be expected to appear between the bands corresponding to the free RNA and the binary complex. However, we did not observe a band of the ternary complex either with this set of samples or in a reciprocal experiment where the radioactive probe *COX2*-58-95 was used at a fixed concentration and the unlabeled probe *COX2*-1-30 was present at

increasing concentrations (Figure 4D). Moreover, each probe appeared to outcompete the other one when added in excess, with the target in the 5'-UTR exhibiting a higher affinity to the protein. Thus, our data suggest that rPet111p can only bind to one RNA target at a time and, therefore, at least some of the RNA recognition and/or binding elements in the protein may be involved in interaction with each of the two targets.

Discussion

Genetic studies in yeast have identified a set of nuclear gene products that activate the translation of mitochondrial mRNAs (2-4). One of these factors, Pet111p, is specifically required for the translation of *COX2* mRNA (6) and was suggested to act by a direct association with the 5'-UTR of the transcript (13). However, this suggestion has not yet been verified experimentally, nor has a mechanism been proposed by which the presumed interaction could lead to the activation of translation. Here, we set out to examine the relationship between Pet111p and *COX2* in greater detail. We found that the protein is indeed associated predominantly with *COX2* *in vivo* (Figure 1) and binds directly to two distinct RNA targets *in vitro* (Figure 3). We mapped the targets to the regions 7-19 (5'-UTR target) and 66-86 (ORF target) relative to the transcription start site (Figure 4A, B). Obviously, not all nucleotides within the mapped boundaries may be critical for the specific binding of Pet111p. The sequences that are actually recognized are expected to be somewhat shorter and may be discontinuous. A comprehensive mutagenesis analysis is needed in order to identify the RNA bases that constitute the actual signals recognized by the protein.

The two identified targets of Pet111p vary in length and do not contain an apparent common sequence pattern that would be stringent enough to set these regions apart from the rest of the mitochondrial RNA. It is not obvious how a single protein can recognize these two diverse targets. Our EMSA data show that the protein can only bind to one of the targets at a time (Figure 4D), which could be either due to a steric overlap of the two RNA binding sites or because some elements in the protein are engaged during the recognition of either target. Alternatively, Pet111p may undergo structural reorganization to adapt to

certain targets, but not others, by an induced fit mechanism. In this scenario, the same structural elements may be involved in different modes of specific binding to each of the two targets depending on the RNA sequence context and the structural configuration of the corresponding RNA recognition modules in the protein.

It is currently unclear how binding of Pet111p may promote the translation of *COX2*. In general, the protein could modify the structure of the message, facilitate the recruitment of the ribosome at the site of initiation, or stabilize the association of the mRNA with other yet unknown factors needed for efficient translation. A recent study has shown that the mitochondrial ribosome cannot associate with *COX2* in Δ *PET111* cells, whereas binding to other mRNAs is not significantly affected (23), however the mechanism behind this effect is unclear. It has been predicted that the 5'-end proximal region in *COX2* may assume the fold shown in Figure 5A (24). In this structure, a sequence in the vicinity of the translation initiation codon is base paired with the upstream RNA. Remarkably, most of the upstream sequence involved in the duplex overlaps with the Pet111p 5'-UTR target mapped in this study. Therefore, binding of Pet111p would prevent the duplex from forming, thus making the translation initiation region single-stranded and accessible to the ribosome. A comprehensive mutagenesis analysis of the *COX2* 5'-UTR has revealed a 31-nt region, located between positions 9 and 39, where substitutions led to a loss of translation of the mutant mRNA and cellular respiration (19). Significantly, the Pet111p 5'-UTR binding target substantially overlaps with the upstream part of this region (Figure 5A). Curiously, the reported mutants demonstrated two clearly distinct phenotypes. Substitutions downstream from position A23 did not significantly destabilize the mutant mRNAs, but inhibited their translation. Conversely, a drastic decrease in the mRNA levels was added to the translational defects when the nucleotides upstream from position C24 were mutated. These latter mutations alter the Pet111p 5'-UTR target and would be expected to interfere with the binding of the protein. Since inactivation of *PET111* was reported to cause up to a 10-fold decrease in levels of *COX2* (6), the observed destabilization of the mutant mRNAs was likely

caused by the loss of protection by Pet111p. The loss of translation resulting from the substitutions (19) and deletions (13) introduced into the 5'-UTR downstream from the Pet111p target suggests that a second enhancer of translation may be present there. This element may function at the RNA level or serve as a binding site for an additional translational activator. Taking all of the above considerations into account, our mapping of the Pet111p 5'-UTR binding target is consistent with results of previous genetic, *in vivo* biochemistry, and structural prediction analysis of the 5'-leader.

The finding that Pet111p contacts *COX2* inside the ORF was surprising, as none of the mRNA-specific yeast mitochondrial translational activators were previously reported to act outside of the 5'-UTRs. Remarkably, the only known mammalian mitochondrial translational activator, TACO1, has recently been shown to bind selectively to the ORF of *COX1* (25). Our data thus indicate that a similar phenomenon may also exist in yeast, and regulation of yeast mitochondrial translation may involve binding of activators inside ORFs. Significantly, translation of a chimeric mRNA, in which the *COX2* ORF was fused to an upstream *COX3* 5'-UTR sequence, was possible in the absence of Pet111p (7). Therefore, if the binding of Pet111p to the ORF target is required for translation in the wild type background, this requirement must be dictated by an element present in the *COX2* 5'-UTR and is bypassed when the entire leader is replaced. However, the functional significance of the binding of Pet111p at this site is yet to be confirmed genetically. Previous work has shown that a positively acting translation control element is embedded in the region that encodes the first 14 amino acids of the Cox2p precursor and that the sequence comprising codons 2 to 6 is critical for the function of this element (20). The sequence of codons 7 to 10 was also important for translation when codon 6 was mutated. Notably, the mapped Pet111p ORF target, which approximately corresponds to codons 5 to 11, partially overlaps with this control element (Figure 5B). The reported translational and respiratory defects induced by mutations within the first 10 codons of *COX2* may therefore result from weakening the interaction between Pet111p and its ORF target. Consistently, these defects were relieved in cells overexpressing Pet111p (20), although an effect of

the overexpression on the interaction of *Pet111p* with the 5'-UTR target might have also contributed to the suppression. The proximal region of the *COX2* ORF was suggested to fold into a structure (20) such that the nucleotides at the site of translation initiation are base paired with a downstream sequence, which is included in the ORF binding target of *Pet111p* (Figure 5B). Therefore, similar to the mechanism suggested in Figure 5A, binding of the protein would be expected to prevent the base pairing of the initiation region, making it available for association with the ribosome. The two putative structures shown in Figure 5 do not appear to be compatible and thus the mRNA may alternate between the two states. Simultaneous binding of two *Pet111p* molecules at both targets may be necessary to prevent base pairing of the translation initiation region. In addition, a translation-inhibiting element has been identified in the sequence comprising codons 15 to 25 (26) and a part of this sequence is predicted to form a stem-loop structure with an upstream region (20) as shown in Figure 5B. Weakening the structure by deletion or substitution of the involved nucleotides diminished the translation-inhibiting effect of this element (20,26). Importantly, the ORF target of *Pet111p* partially overlaps with the sequence of the upstream strand of the stem of the structure. Therefore, binding of the protein should interfere with the formation of the structure, thereby providing additional means to promote *COX2* translation. While the proposed model of translational activation by *Pet111p* is certainly speculative, it is remarkable that a very similar mechanism has been shown to facilitate the translation of mRNA in maize chloroplasts. In this mechanism, binding of PPR10 in the 5'-UTR of *ATP-H* induces structural remodeling in the initiation region, which liberates the Shine-Dalgarno sequence and thus enables translation (27).

Based on bioinformatic analysis, *Pet111p* has been assigned as a member of the pentatricopeptide repeat (PPR) protein family (28). Especially numerous in plant organelles (29), PPR proteins generally function in post-transcriptional RNA metabolism by associating with predominantly single-stranded RNA targets in a sequence-specific manner (30). Plant PPR proteins recognize their targets using domains composed of

multiple 35-amino acid PPR motifs. The recognition occurs in a modular mode, at a ratio of one RNA base per one PPR motif, and in accordance with a set of principles known as the PPR code (31). Only three *S. cerevisiae* proteins (*Aep3p*, *Dmr1p*, and *Pet309p*) were found to contain the sequence motifs that matched the plant PPR pattern (32). Although the general functional profile of a group of 12 additional PPR proteins identified in yeast (28) appears to be consistent with that of the plant PPR proteins, the sequence signature of their PPR motifs is evidently distinct (33). It is therefore not clear whether the yeast PPR proteins utilize the same mechanistic patterns as those in plants. Our data indicate that *Pet111p*, a protein from the yeast PPR subfamily, can interact with single-stranded RNA directly and sequence-specifically. However, it remains to be determined whether this recognition utilizes a PPR code similar to the one in plants and if it is modular in nature. To better understand the function of yeast PPR proteins, more information on the corresponding protein-RNA interacting pairs is needed. Other gene-specific translational activators that are presumed to selectively interact with targets in the yeast mitochondrial mRNAs have been classified as PPR proteins (28). The approach presented in this work opens a way to mapping the targets of these proteins with high precision.

Experimental procedures

Oligonucleotides

Synthetic DNA oligonucleotides were purchased from Integrated DNA Technology (IDT) and synthetic RNA was from GE Healthcare Dharmacon and IDT (sequences are listed in Table S1). The RNA probes used in the EMSA and RNase footprinting experiments were 5'-labeled and gel-purified as described in Supporting Information.

PAR-CLIP analysis

PAR-CLIP and data acquisition were performed as described in Supporting Information. Data quality control and mapping was performed as described (34). Briefly, sequencing reads were quality trimmed and mapped to the *S. cerevisiae* genome (sacCer3, version 64.2.1) using the short read aligner STAR version 2.5.2b (35). Coverage

plots were generated using GenomicAlignments (36).

Determination of the mature N-terminus of Pet111p

Mitochondria were isolated from yeast expressing tagged *Pet111p* as specified in Supporting Information. Approximately 0.3 ml of settled mitochondria were resuspended in 1.2 ml of lysis solution (7 M guanidine-HCl, 100 mM NaCl, 15 mM imidazole, 3 mM β -mercaptoethanol (β -ME)) and the suspension was sonicated on ice with five 30 sec pulses intermitted with 30 sec pauses on a F60 sonic dismembrator (Fisher Scientific). The lysate was cleared by centrifugation (20,000 \times g, 15 min) and the supernatant was incubated with 20 μ l of Ni-IDA agarose beads (Gold Biotechnology) in a tumbling tube overnight at room temperature. The beads were then washed three times with the lysis solution and two times with water using 1.4 ml per wash. The bound proteins were eluted with 80 μ l of 1 \times lithium dodecyl sulfate (LDS) gel loading buffer (Novex, Life technologies), a 20 μ l sample of the eluate was separated by 4-12 % LDS PAGE, and the protein bands were visualized by coomassie staining. The band that corresponded to the tagged *Pet111p* was identified by PMF as described in Supporting Information. The eluted proteins were separated by PAGE once again, transferred onto an Immobilon-PSQ membrane (EMD Millipore) by electroblotting, and the tagged *Pet111p* band was cut out from the membrane and submitted for N-terminal sequencing (Midwest Analytical).

Expression and purification of rPet111p

E. coli XJb(DE3) cells (Zymo Research) were transformed with plasmid pGD1 and r*Pet111p* was expressed at a temperature of 12 °C. The protein was purified sequentially on a Ni-agarose column, by heparin affinity chromatography, and gel filtration as described in Supporting Information.

Mapping of the 5'-end in mature COX2

DNA primer COX2-96-76 was hybridized to *COX2* in a preparation of total mitochondrial RNA and extended with RT as detailed in Supporting Information.

Electrophoretic mobility shift assays

r*Pet111p* was combined with 5'-[³²P]-labeled RNA probes (0.1 μ M) in 10 μ l of binding buffer (20 mM Tris-HCl pH 7.2, 50 mM NaCl, 5 mM MgCl₂, 5 % glycerol). Yeast tRNA (Sigma) was added at a two-fold molar excess over the protein (or 1 μ M in Figure 4D) to reduce nonspecific binding and the mixtures were incubated for 20 min at 30 °C. The mixtures were supplemented with 2 μ l of 30 % glycerol spiked with xylene cyanol and bromophenol blue, and loaded on 8 % (37.5:1, acrylamide:bisacrylamide) polyacrylamide gels cast in the presence of 1 \times Tris/borate/EDTA (TBE) buffer. Electrophoresis was performed at room temperature in 0.5 \times TBE running buffer for 15 min at 175 V. Radioactive bands corresponding to protein-RNA complexes and unbound RNA were visualized using storage phosphor screens and a Typhoon 9410 scanner (GE Healthcare).

RNase footprinting

5'-[³²P]-labeled RNA probes were incubated with r*Pet111p* (where indicated) in 10 μ l of binding buffer (specified above) for 20 min at 30 °C. Yeast tRNA (1 μ M and 1.2 μ M in the experiments shown in Figure 4A and Figure 4B, respectively) was present in the mixtures. RNase I (New England Biolabs) was then added to a concentration of 8 units (U)/ml where indicated and the mixtures were incubated for 16 min at 30 °C. RNase A (Qiagen) was used at a concentration of 0.8 ng/ml where indicated. The reactions were stopped by mixing them with 10 μ l of gel loading buffer (50 mM EDTA in 95 % formamide spiked with xylene cyanol and bromophenol blue) and heating at 95 °C for 5 min. The products of digestion were separated in gradient thickness (0.4 mm to 1.2 mm) 20 % (19:1, acrylamide:bisacrylamide) gels cast with 7 M urea. The radioactive RNA species were visualized by phosphor imaging with a Typhoon 9410 scanner (GE Healthcare) and quantified using ImageQuant 5.2 software (Molecular Dynamics).

Acknowledgements: PAR-CLIP sequencing data were deposited to the NCBI Gene Expression Omnibus (GSE117899). We thank William McAllister for critically reading the manuscript and useful suggestions. We also thank Claire Corbett and Gary Devine for technical assistance during initial stages of this project.

Conflict of interest: The authors declare that they have no conflicts of interest with the contents of this article.

References

1. Strecker, V., Kadeer, Z., Heidler, J., Cruciat, C.-M., Angerer, H., Giese, H., Pfeiffer, K., Stuart, R. A., and Wittig, I. (2016) Supercomplex-associated Cox26 protein binds to cytochrome c oxidase. *Biochimica et Biophysica Acta (BBA) - Molecular Cell Research* **1863**, 1643-1652
2. Ott, M., Amunts, A., and Brown, A. (2016) Organization and regulation of mitochondrial protein synthesis. *Annual Review of Biochemistry* **85**, 77-101
3. Herrmann, J. M., Woellhaf, M. W., and Bonnefoy, N. (2013) Control of protein synthesis in yeast mitochondria: The concept of translational activators. *Biochimica et Biophysica Acta (BBA) - Molecular Cell Research* **1833**, 286-294
4. Fox, T. D. (2012) Mitochondrial protein synthesis, import, and assembly. *Genetics* **192**, 1203-1234
5. Strick, C. A., and Fox, T. D. (1987) *Saccharomyces cerevisiae* positive regulatory gene PET111 encodes a mitochondrial protein that is translated from an mRNA with a long 5' leader. *Molecular and Cellular Biology* **7**, 2728-2734
6. Poutre, C. G., and Fox, T. D. (1987) PET111, a *Saccharomyces cerevisiae* nuclear gene required for translation of the mitochondrial mRNA encoding cytochrome c oxidase subunit II. *Genetics* **115**, 637-647
7. Mulero, J. J., and Fox, T. D. (1993) Pet111 Acts in the 5'-leader of the *Saccharomyces cerevisiae* mitochondrial Cox2 mRNA to promote its translation. *Genetics* **133**, 509-516
8. Green-Willms, N. S., Butler, C. A., Dunstan, H. M., and Fox, T. D. (2001) Pet111p, an inner membrane-bound translational activator that limits expression of the *Saccharomyces cerevisiae* mitochondrial gene COX2. *Journal of Biological Chemistry* **276**, 6392-6397
9. Sanchirico, M. E., Fox, T. D., and Mason, T. L. (1998) Accumulation of mitochondrially synthesized *Saccharomyces cerevisiae* Cox2p and Cox3p depends on targeting information in untranslated portions of their mRNAs. *The EMBO Journal* **17**, 5796-5804
10. Naithani, S., Saracco, S. A., Butler, C. A., and Fox, T. D. (2003) Interactions among COX1, COX2, and COX3 mRNA-specific translational activator proteins on the inner surface of the mitochondrial inner membrane of *Saccharomyces cerevisiae*. *Molecular Biology of the Cell* **14**, 324-333
11. Krause, K., Lopes de Souza, R., Roberts, D. G. W., and Dieckmann, C. L. (2004) The mitochondrial message-specific mRNA protectors Cbp1 and Pet309 are associated in a high-molecular weight complex. *Molecular Biology of the Cell* **15**, 2674-2683
12. Kehrein, K., Schilling, R., Möller-Hergt, B. V., Wurm, C. A., Jakobs, S., Lamkemeyer, T., Langer, T., and Ott, M. (2015) Organization of mitochondrial gene expression in two distinct ribosome-containing assemblies. *Cell Reports* **10**, 843-853
13. Mulero, J. J., and Fox, T. D. (1993) Alteration of the *Saccharomyces cerevisiae* COX2 mRNA 5'-untranslated leader by mitochondrial gene replacement and functional interaction with the translational activator protein PET111. *Molecular Biology of the Cell* **4**, 1327-1335
14. Gelperin, D. M., White, M. A., Wilkinson, M. L., Kon, Y., Kung, L. A., Wise, K. J., Lopez-Hoyo, N., Jiang, L., Piccirillo, S., Yu, H., Gerstein, M., Dumont, M. E., Phizicky, E. M., Snyder, M., and Grayhack, E. J. (2005) Biochemical and genetic analysis of the yeast proteome with a movable ORF collection. *Genes & Development* **19**, 2816-2826
15. Henzel, W. J., Watanabe, C., and Stults, J. T. (2003) Protein identification: the origins of peptide mass fingerprinting. *Journal of the American Society for Mass Spectrometry* **14**, 931-942
16. Wiesenberger, G., and Fox, T. D. (1997) Pet127p, a membrane-associated protein involved in stability and processing of *Saccharomyces cerevisiae* mitochondrial RNAs. *Molecular and Cellular Biology* **17**, 2816-2824
17. Coruzzi, G., Bonitz, S. G., Thalenfeld, B. E., and Tzagoloff, A. (1981) Assembly of the mitochondrial membrane system. Analysis of the nucleotide sequence and transcripts in the *oxi1* region of yeast mitochondrial DNA. *Journal of Biological Chemistry* **256**, 12780-12787

18. Costanzo, M. C., Bonnefoy, N., Williams, E. H., Clark-Walker, G. D., and Fox, T. D. (2000) Highly diverged homologs of *Saccharomyces cerevisiae* mitochondrial mRNA-specific translational activators have orthologous functions in other budding yeasts. *Genetics* **154**, 999-1012
19. Dunstan, H. M., Green-Willms, N. S., and Fox, T. D. (1997) In vivo analysis of *Saccharomyces cerevisiae* COX2 mRNA 5'-untranslated leader functions in mitochondrial translation initiation and translational activation. *Genetics* **147**, 87-100
20. Bonnefoy, N., Bsat, N., and Fox, T. D. (2001) Mitochondrial translation of *Saccharomyces cerevisiae* COX2 mRNA is controlled by the nucleotide sequence specifying the pre-Cox2p leader peptide. *Molecular and Cellular Biology* **21**, 2359-2372
21. Nilsen, T. W. (2014) RNase Footprinting to Map Sites of RNA-Protein Interactions. *Cold Spring Harbor Protocols* **2014**, pdb.prot080788
22. Meador, J., Cannon, B., Cannistraro, V. J., and Kennell, D. (1990) Purification and characterization of *Escherichia coli* RNase I. *European Journal of Biochemistry* **187**, 549-553
23. Couvillion, M. T., Soto, I. C., Shipkovenska, G., and Churchman, L. S. (2016) Synchronized mitochondrial and cytosolic translation programs. *Nature* **533**, 499-503
24. Papadopoulou, B., Dekker, P., Blom, J., and Grivell, L. A. (1990) A 40 kd protein binds specifically to the 5'-untranslated regions of yeast mitochondrial mRNAs. *The EMBO Journal* **9**, 4135-4143
25. Richman, T. R., Spåhr, H., Ermer, J. A., Davies, S. M. K., Viola, H. M., Bates, K. A., Papadimitriou, J., Hool, L. C., Rodger, J., Larsson, N.-G., Rackham, O., and Filipovska, A. (2016) Loss of the RNA-binding protein TACO1 causes late-onset mitochondrial dysfunction in mice. *Nature Communications* **7**, 11884
26. Williams, E. H., and Fox, T. D. (2003) Antagonistic signals within the COX2 mRNA coding sequence control its translation in *Saccharomyces cerevisiae* mitochondria. *RNA* **9**, 419-431
27. Prikryl, J., Rojas, M., Schuster, G., and Barkan, A. (2011) Mechanism of RNA stabilization and translational activation by a pentatricopeptide repeat protein. *Proceedings of the National Academy of Sciences* **108**, 415-420
28. Lipinski, K. A., Puchta, O., Surendranath, V., Kudla, M., and Golik, P. (2011) Revisiting the yeast PPR proteins—application of an iterative hidden Markov model algorithm reveals new members of the rapidly evolving family. *Molecular Biology and Evolution* **28**, 2935-2948
29. Schmitz-Linneweber, C., and Small, I. (2008) Pentatricopeptide repeat proteins: a socket set for organelle gene expression. *Trends in Plant Science* **13**, 663-670
30. Barkan, A., and Small, I. (2014) Pentatricopeptide repeat proteins in plants. *Annual Review of Plant Biology* **65**, 415-442
31. Barkan, A., Rojas, M., Fujii, S., Yap, A., Chong, Y. S., Bond, C. S., and Small, I. (2012) A combinatorial amino acid code for RNA recognition by pentatricopeptide repeat proteins. *PLoS Genetics* **8**, e1002910
32. Small, I. D., and Peeters, N. (2000) The PPR motif - a TPR-related motif prevalent in plant organellar proteins. *Trends in Biochemical Sciences* **25**, 46-47
33. Herbert, C. J., Golik, P., and Bonnefoy, N. (2013) Yeast PPR proteins, watchdogs of mitochondrial gene expression. *RNA Biology* **10**, 1477-1494
34. Baejen, C., Torkler, P., Gressel, S., Essig, K., Söding, J., and Cramer, P. (2014) Transcriptome Maps of mRNP Biogenesis Factors Define Pre-mRNA Recognition. *Molecular Cell* **55**, 745-757
35. Dobin, A., Davis, C. A., Schlesinger, F., Drenkow, J., Zaleski, C., Jha, S., Batut, P., Chaisson, M., and Gingeras, T. R. (2013) STAR: ultrafast universal RNA-seq aligner. *Bioinformatics* **29**, 15-21
36. Lawrence, M., Huber, W., Pagès, H., Aboyoun, P., Carlson, M., Gentleman, R., Morgan, M. T., and Carey, V. J. (2013) Software for Computing and Annotating Genomic Ranges. *PLoS Computational Biology* **9**, e1003118

37. Fukasawa, Y., Tsuji, J., Fu, S.-C., Tomii, K., Horton, P., and Imai, K. (2015) MitoFates: improved prediction of mitochondrial targeting sequences and their cleavage sites. *Molecular & Cellular Proteomics* **14**, 1113-1126
38. Osinga, K. A., De Vries, E., Van der Horst, G., and Tabak, H. F. (1984) Processing of yeast mitochondrial messenger RNAs at a conserved dodecamer sequence. *The EMBO Journal* **3**, 829-834

FOOTNOTES

This work was supported by New Jersey Health Foundation grant to M.A. (PC127-13). J.L.J. acknowledges the support from Rowan University Graduate School of Biomedical Sciences.

The abbreviations used are: 4tU, 4-thiouracil; β -ME, β -mercaptoethanol; COX, cytochrome *c* oxidase; EMSA, electrophoretic mobility shift assay; IP, immunoprecipitation; LDS, lithium dodecyl sulfate; MPP, mitochondrial processing peptidase; mtDNA, mitochondrial DNA; nt, nucleotide; PAR-CLIP, photoactivatable ribonucleoside-enhanced crosslinking and immunoprecipitation; PPR, pentatricopeptide repeat; PMF, peptide mass fingerprinting; PMSF, phenylmethanesulfonyl fluoride; PNK, polynucleotide kinase; RT, reverse transcriptase; TAP, tandem affinity purification; TBE, Tris/borate/EDTA; U, unit of activity

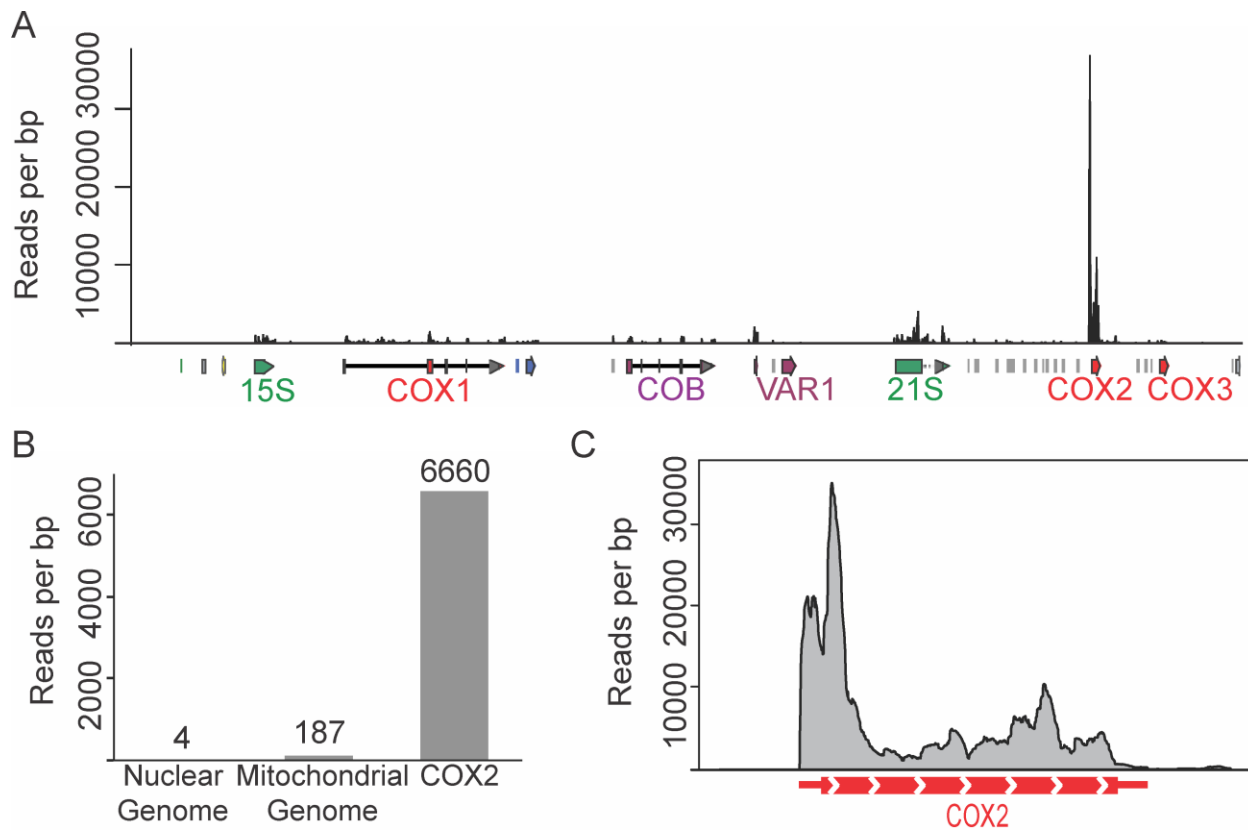


Figure 1. *Pet111p* is predominantly associated with *COX2* mRNA *in vivo*. (A) PAR-CLIP analysis of cells expressing *Pet111p*-TAP was performed and the resulting RNA reads were aligned to the yeast mitochondrial genomic sequence. (B) The abundance of the RNA reads associated with the nuclear and mitochondrial genomic sequences was compared to that of the *COX2*-associated reads. (C) A portion of the alignment in panel A showing the distribution of the sequencing reads in the vicinity of the *COX2* gene. The position of the coding sequence is indicated by the red bar with the arrows showing the direction of translation. The red lines correspond to the untranslated regions of the mature mRNA.

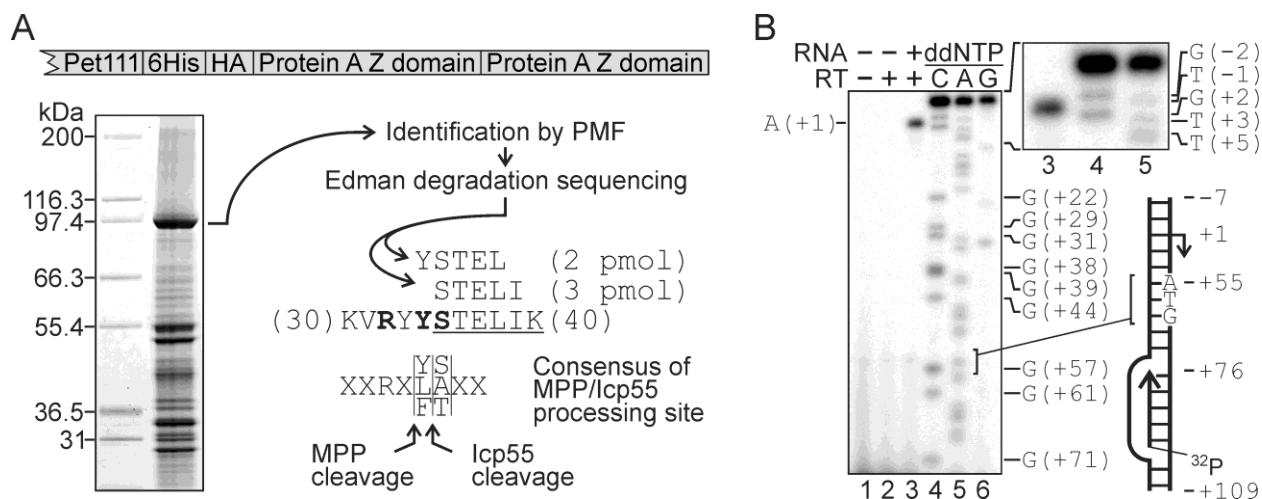


Figure 2. Characterization of the processing of *Pet111p* and *COX2* in mitochondria. (A) An image of a coomassie-stained polyacrylamide gel showing the proteins in a preparation of tagged *Pet111p* partially purified from yeast mitochondria. The composition of the C-terminal purification tag is shown above the image. The positions of the hexahistidine (6His) and hemagglutinin epitope (HA) tags are indicated. The protein in the indicated band was identified as *Pet111p* by PMF and Edman degradation analysis of the protein revealed two sequence reads, pointed to by the bent arrows. The reads are aligned with a portion of the *Pet111p* sequence (numbers indicate positions of the flanking amino acid in the sequence of the *Pet111p* precursor), in which the determined N-terminal sequence of the mature protein is underlined. The amino acids in boldface match the consensus of the MPP/Icp55 processing site (37), which is shown below the alignment. The sites of cleavage by MPP and Icp55 are indicated by arrows. (B) A phosphorimaging scan of an area of a polyacrylamide gel showing the products of extension of a 5'-³²P]-labeled DNA primer *COX2*-96-76. The primer was hybridized to *COX2* mRNA in a total mitochondrial RNA isolate and extended with RT (lane 3). Control lanes 1 and 2 contained, respectively, the unextended primer and the primer extended in the absence of mitochondrial RNA. The length of the product of extension in lane 3 was determined by a comparison with DNA size markers (lanes 4-6). The markers were generated by extension of the primer in the presence of ddNTPs as specified above the image. The double-stranded DNA template used in the primer extension reactions contained a sequence of the *COX2* promoter between positions -7 and +109 relative to the start-site (+1), as explained by the scheme to the right. The bands in lane 4 are assigned on the right of the image and the position on the gel that corresponds to the initiation codon is indicated by brackets. An area on the top of the image is enlarged to show the slow-running bands in lanes 3-5 more clearly and the bands in lanes 4 and 5 are assigned on the right. Comparison with the size markers indicates that the 3'-end of the product of primer extension in lane 3 corresponds to position +1.

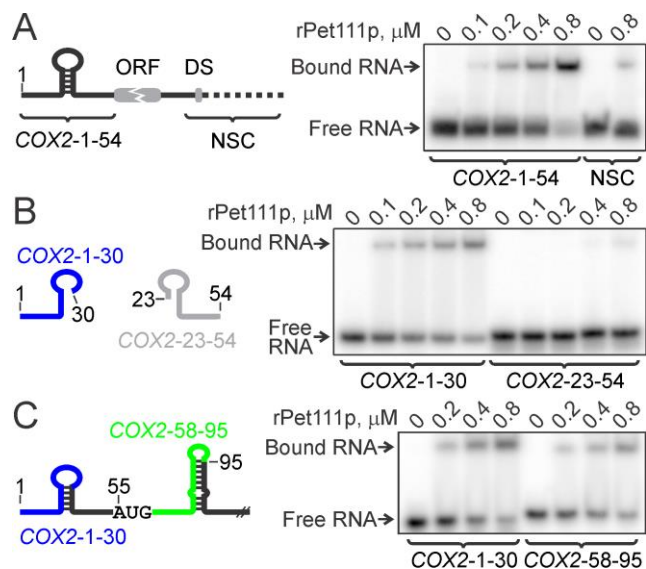


Figure 3. rPet111p binds to specific regions of *COX2* mRNA *in vitro*. The labeled RNA probes shown in the schemes to the left were incubated with varying concentrations of rPet111p and resolved by native PAGE. (A) The binding efficiency of two probes was compared, one spanning the entire 5'-UTR and the other corresponding to a sequence downstream of the ORF (NSC). DS marks the position of a conserved dodecameric sequence (38) and the dashed line indicates the region not present in the mature *COX2* (17). (B) Two overlapping probes were designed to cover the sequence of the 5'-UTR and their interaction with rPet111p was compared. (C) The binding efficiency of the *COX2*-1-30 probe was compared to that of a probe (*COX2*-58-95) representing a sequence in the beginning of the ORF.

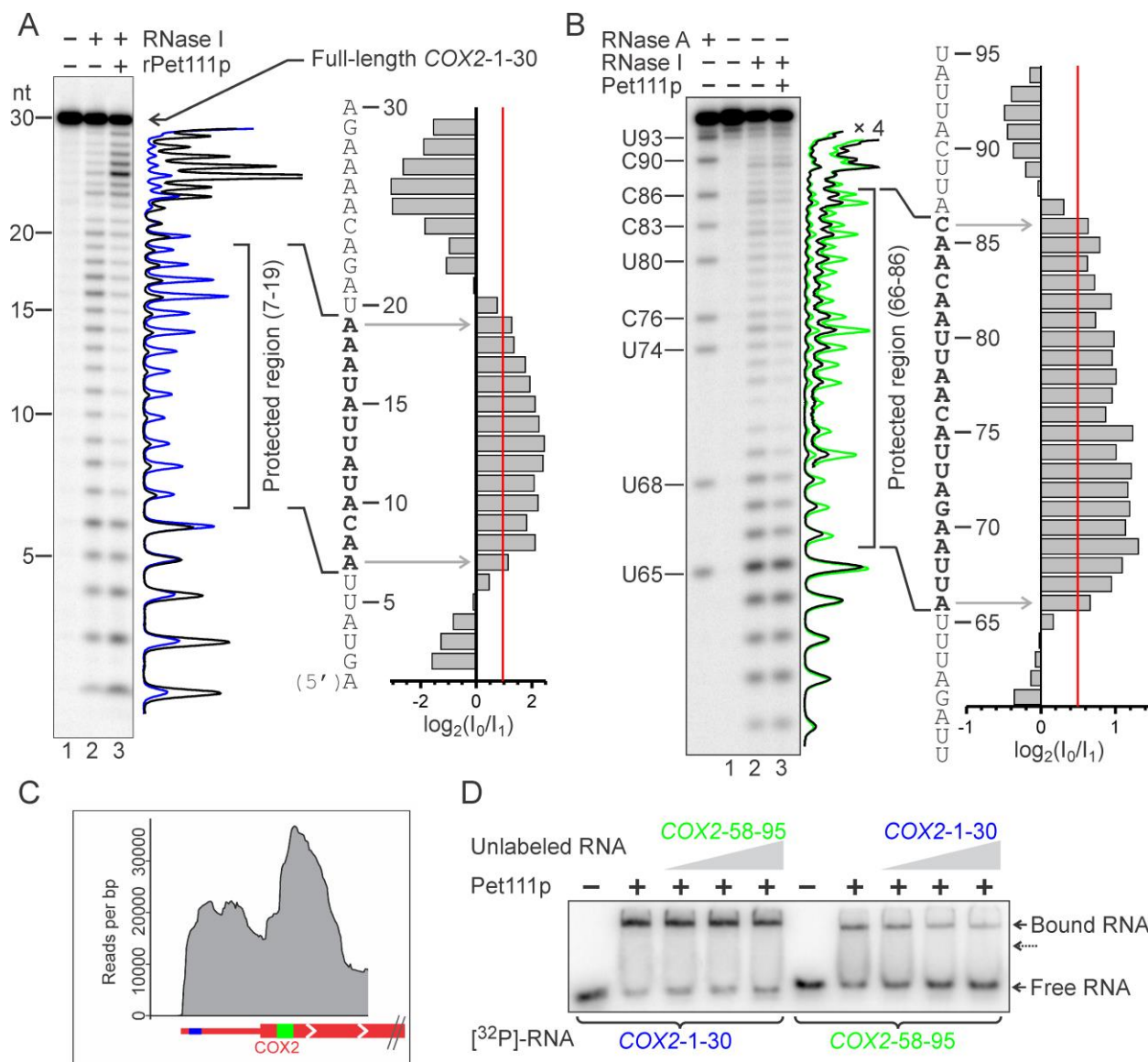


Figure 4. rPet111p recognizes two distinct targets in the 5'-end proximal region of *COX2* mRNA. (A) 5'-[³²P]-labeled *COX2*-1-30 RNA (0.6 μ M) was digested with RNase I in the absence or presence of rPet111p (0.8 μ M). The cleavage products were resolved by denaturing PAGE. The traces represent the distribution of radioactivity within lanes 2 (blue) and 3 (black). For each RNA fragment 2 to 29 nt in length, intensities of the corresponding bands in lanes 2 (I_0) and 3 (I_1) are plotted as $\log_2(I_0/I_1)$. Positions in the RNA, at which the bars in the plot exceeded 55 % of the average of all positive-value bars (red line) were considered protected by rPet111p and are indicated by boldface in the sequence of *COX2*-1-30. (B) 5'-[³²P]-labeled *COX2*-58-95 (0.3 μ M) was treated with RNase I in the absence or presence of rPet111p (0.6 μ M) and the digestion products were resolved by PAGE. Digestion with RNase A was performed to generate RNA size markers (left lane). The traces and the bar plot on the right are as in panel A. The green and black traces correspond to lanes 2 and 3, respectively. (C) A region of the alignment of the PAR-CLIP reads (Figure 1) is shown. The positions of the two identified targets of rPet111p are indicated in blue (5'-UTR) and green (ORF). (D) 5'-[³²P]-labeled *COX2*-1-30 was incubated with 0.8 μ M rPet111p. The formed complex was resolved from the unbound probe in a native gel. Where indicated, unlabeled *COX2*-58-95 was present in the mixtures (0.2, 0.4, and 0.8 μ M). In a reciprocal experiment (the right side

of the image), the labeled probe was *COX2-58-95* and the unlabeled competitor was *COX2-1-30*. The dotted arrow points to the expected position of rPet111p bound to both RNA probes.

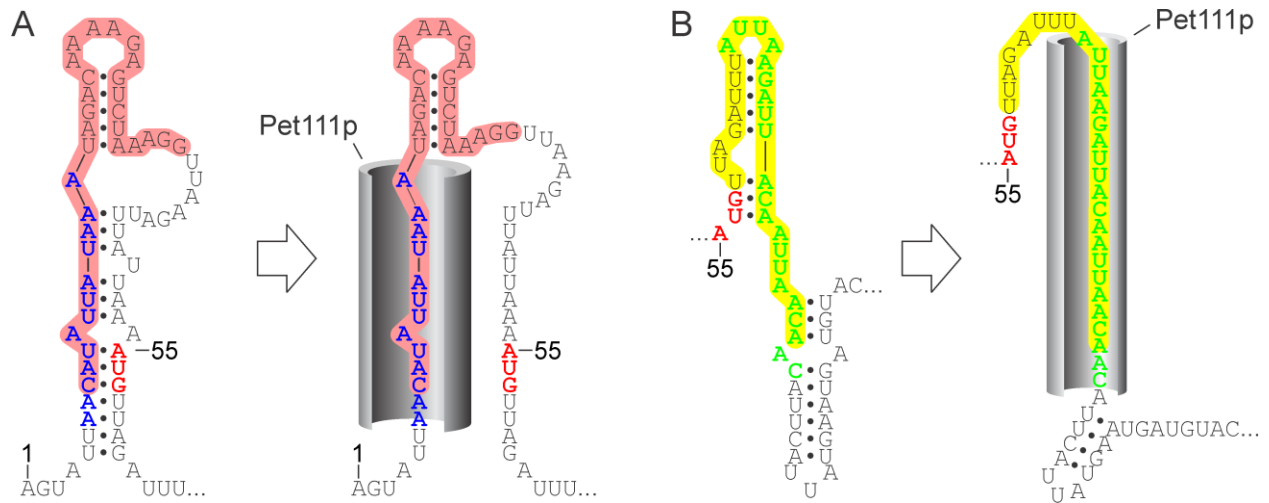


Figure 5. A possible mechanism of activation of *COX2* translation by *Pet111p*. (A) A structure formed by the 5'-UTR and a region in the beginning of the ORF as previously proposed (24) is shown on the left. The blue lettering indicates the UTR target of r*Pet111p*. The region highlighted in pink contains residues required for respiration (19). (B) A previously suggested alternative structure involving the beginning of the ORF is shown on the left (20). The *Pet111p* ORF target is shown in green lettering. Deletions or substitutions of certain nucleotides within the sequence highlighted in yellow, either in the WT or 70A>C;72A>U background, disrupted translation (20). On the right of both panels, it is shown how binding of *Pet111p* (grey hollow cylinders) to corresponding targets would prevent the RNA structures from forming, making the region of the start codon (red lettering) single-stranded and available for translation. Binding of *Pet111p* at the ORF target is also expected to interfere with a downstream stem-loop structure (panel B). Destabilization of this structure was reported to promote translation of *COX2* (20).

Yeast mitochondrial protein Pet111p binds directly to two distinct targets in *COX2* mRNA, suggesting a mechanism of translational activation

Julia L. Jones, Katharina B. Hofmann, Andrew T. Cowan, Dmitry Temiakov, Patrick Cramer and Michael Anikin

J. Biol. Chem. published online March 25, 2019

Access the most updated version of this article at doi: [10.1074/jbc.RA118.005355](https://doi.org/10.1074/jbc.RA118.005355)

Alerts:

- [When this article is cited](#)
- [When a correction for this article is posted](#)

[Click here](#) to choose from all of JBC's e-mail alerts